ISSN 1726-5749

SENSORS & TRANSDUCERS

vol. 90
Special
4/08

Modern Sensing Technologies

International Frequency Sensor Association Publishing

IFSA

Sensors & Transducers

Special Issue
April 2008

www.sensorsportal.com

ISSN 1726-5479

Sensors & Transducers Journal (ISSN 1726-5479) is a peer review international journal published monthly online by International Frequency Sensor Association (IFSA). Available in electronic and CD-ROM.

Sensors & Transducers Journal

Contents

Volume 90
Special Issue
April 2008

www.sensorsportal.com

ISSN 1726-5479

Special Issue on Modern Sensing Technologies

Editorial

Modern Sensing Technologies
Subhas Chandra Mukhopadhyay and Gourab Sen Gupta I

Sensors for Medical/Biological Applications

Characteristics and Application of CMC Sensors in Robotic Medical and Autonomous Systems
X. Chen, S. Yang, H. Natuhara K. Kawabe, T. Takemitu and S. Motojima 1

SGFET as Charge Sensor: Application to Chemical and Biological Species Detection
T. Mohammed-Brahim, A.-C. Salaün, F. Le Bihan 11

Estimation of Low Concentration Magnetic Fluid Weight Density and Detection inside an Artificial Medium Using a Novel GMR Sensor
Chinthaka Gooneratne, Agnieszka Łekawa, Masayoshi Iwahara, Makiko Kakikawa and Sotoshi Yamada 27

Design of an Enhanced Electric Field Sensor Circuit in 0.18 µm CMOS for a Lab-on-a-Chip Bio-cell Detection Micro-Array
S. M. Rezaul Hasan and Siti Noorjannah Ibrahim 39

Wireless Sensors

Coexistence of Wireless Sensor Networks in Factory Automation Scenarios
Paolo Ferrari, Alessandra Flammini, Daniele Marioli, Emiliano Sisinni, Andrea Taroni 48

Wireless Passive Strain Sensor Based on Surface Acoustic Wave Devices
T. Nomura, K. Kawasaki and A. Saitoh 61

Environmental Measurement OS for a Tiny CRF-STACK Used in Wireless Network
Vasanth Iyer, G. Rammurthy, M. B. Srinivas 72

Ubiquitous Healthcare Data Analysis And Monitoring Using Multiple Wireless Sensors for Elderly Person
Sachin Bhardwaj, Dae-Seok Lee, S.C. Mukhopadhyay and Wan-Young Chung 87

Capacitive Sensors

Resistive and Capacitive Based Sensing Technologies
Winncy Y. Du and Scott W. Yelich 100

A Versatile Prototyping System for Capacitive Sensing
Daniel Hrach, Hubert Zangl, Anton Fuchs and Thomas Bretterklieber 117

The Physical Basis of Dielectric Moisture Sensing
J. H. Christie and I. M. Woodhead 128

Sensors Signal Processing

Kalman Filter for Indirect Measurement of Electrolytic Bath State Variables: Tuning Design and Practical Aspects
Carlos A. Braga, Joâo V. da Fonseca Neto, Nilton F. Nagem, Jorge A. Farid and Fábio Nogueira da Silva 139

Signal Processing for the Impedance Measurement on an Electrochemical Generator
El-Hassane Aglzim, Amar Rouane, Mustapha Nadi and Djilali Kourtiche 150

Gas Sensors

Gas Sensing Performance of Pure and Modified BST Thick Film Resistor
G. H. Jain, V. B. Gaikwad, D. D. Kajale, R. M. Chaudhari, R. L. Patil, N. K. Pawar, M. K. Deore, S. D. Shinde and L. A. Patil 160

Zirconia Oxygen Sensor for the Process Application: State-of-the-Art
Pavel Shuk, Ed Bailey, Ulrich Guth 174

Image Sensors

Measurement of Digital Camera Image Noise for Imaging Applications
Kenji Irie, Alan E. McKinnon, Keith Unsworth, Ian M. Woodhead 185

Calibration-free Image Sensor Modelling Using Mechanistic Deconvolution
Shen Hin Lim, Tomonari Furukawa 195

Miscellaneous

Functional Link Neural Network-based Intelligent Sensors for Harsh Environments
Jagdish C. Patra, Goutam Chakraborty and Subhas Mukhopadhyay 209

MEMS Based Pressure Sensors – Linearity and Sensitivity Issues
Jaspreet Singh, K. Nagachenchaiah, M. M. Nayak 221

Slip Validation and Prediction for Mars Exploration Rovers
Jeng Yen 233

Actual Excitation-Based Rotor Position Sensing in Switched Reluctance Drives
Ibrahim Al-Bahadly 243

A Portable Nuclear Magnetic Resonance Sensor System
R. Dykstra, M. Adams, P. T. Callaghan, A. Coy, C. D. Eccles, M. W. Hunter, T. Southern, R. L. Ward 255

A Special Vibration Gyroscope
Wang Hong-wei, Chee Chen-jie, Teng Gong-qing, Jiang Shi-yu 267

An Improved CMOS Sensor Circuit Using Parasitic Bipolar Junction Transistors for Monitoring the Freshness of Perishables
S. M. Rezaul Hasan and Siti Noorjannah Ibrahim 276

Sensing Technique Using Laser-induced Breakdown Spectroscopy Integrated with Micro-droplet Ejection System
Satoshi Ikezawa, Muneaki Wakamatsu, Joanna Pawłat and Toshitsugu Ueda 284

A Forward Solution for RF Impedance Tomography in Wood
Ian Woodhead, Nobuo Sobue, Ian Platt, John Christie.. 294

A Micromachined Infrared Senor for an Infrared Focal Plane Array
Seong M. Cho, Woo Seok Yang, Ho Jun Ryu, Sang Hoon Cheon, Byoung-Gon Yu, Chang Auck Choi.. 302

Slip Prediction through Tactile Sensing
Somrak Petchartee and Gareth Monkman.. 310

Broadband and Improved Radiation Characteristics of Aperture-Coupled Stacked Microstrip Antenna for Mobile Communications
Sajal Kumar Palit 325

The Use of Bragg Gratings in the Core and Cladding of Optical Fibres for Accurate Strain Sensing
Ian G. Platt and Ian M. Woodhead 333

Authors are encouraged to submit article in MS Word (doc) and Acrobat (pdf) formats by e-mail: editor@sensorsportal.com
Please visit journal's webpage with preparation instructions: http://www.sensorsportal.com/HTML/DIGEST/Submition.htm

Sensors & Transducers Journal, Vol. 90, Special Issue, April 2008, pp. 27-38

www.sensorsportal.com

Sensors & Transducers

ISSN 1726-5479

http://www.sensorsportal.com

Estimation of Low Concentration Magnetic Fluid Weight Density and Detection inside an Artificial Medium Using a Novel GMR Sensor

Chinthaka GOONERATNE, [*]Agnieszka ŁEKAWA, Masayoshi IWAHARA, Makiko KAKIKAWA and Sotoshi YAMADA

Kanazawa University, Kakuma-machi, Kanazawa, Ishikawa 920-1192, Japan

[*]Lublin University of Technology, Lublin, Poland

E-mail: chinthaka.gooneratne@gmail.com, yamada@magstar.ec.t.kanazawa-u.ac.jp

Received: 15 October 2007 /Accepted: 20 February 2008 /Published: 15 April 2008

Abstract: Hyperthermia treatment has been gaining momentum in the past few years as a possible method to manage cancer. Cancer cells are different to normal cells in many ways including how they react to heat. Due to this difference it is possible for hyperthermia treatment to destroy cancer cells without harming the healthy normal cells surrounding the tumor. Magnetic particles injected into the body generate heat by hysteresis loss and temperature is increased when a time varying external magnetic field is applied. Successful treatment depends on how efficiently the heat is controlled. Thus, it is very important to estimate the magnetic fluid density in the body. Experimental apparatus designed for testing, numerical analysis, and results obtained by experimentation using a simple yet novel and minimally invasive needle type spin-valve giant magnetoresistance (SV-GMR) sensor, to estimate low concentration magnetic fluid weight density and detection of magnetic fluid in a reference medium is reported. *Copyright © 2008 IFSA.*

Keywords: Hyperthermia treatment, SV-GMR sensor, Low-invasive, Magnetic fluid, Demagnetizing factor

---

1. Introduction

The utilization of magnetic nanoparticles has been proposed for a diverse range of potential applications such as in the fields of electronics, biomedicine, energy, military uses and waste management, for several years. With the recent advancements in nanotechnology, smart sensors have been used extensively in explicit biomedical applications [1]. Hyperthermia treatment has the potential to be an effective tool for healing cancer. The principle behind hyperthermia treatment lies in the fact that cancer cells are more sensitive to heat than normal healthy cells [2]. While it has been known for some time that heat does shrink tumors it is only recently that safe ways have been found to raise body temperature in a safe and effective manner. Thus, hyperthermia treatment can be used effectively to kill or weaken cancer cells with negligible effects on healthy cells. The many advantages of this type of treatment include no side effects or pain for the patient, minimally invasive and less treatment time, compared to treatments such as chemotherapy and radiotherapy, and even though the cancer cells do not die completely they may be become more susceptible to treatments such as ionizing radiation or chemotherapy, allowing such therapy to be given in small doses [3].

Magnetic fluid with magnetic nano-particles is injected into the affected area. Magnetic particles generate heat by hysteresis loss and temperature is increased when a time varying external magnetic field is applied [4]. The movement of the magnetic particles can be controlled by external magnetic fields, which means it can be directed to an area of interest, held there until treatment concludes and then removed. As a result of external magnetic fields the temperature of the magnetic nano-particles increases, due to eddy current loss [5]. Given sufficient heat it is possible to destroy or partly destroy cancer cells in the affected area. The amount of nano-particles inside the body must be verified before treatment so that healthy cells won't be affected.

Once the magnetic fluid is injected it spreads throughout the tissue decreasing the content density. Magnetic density is then needed to be confirmed once inside the tissue. The needle type spin valve giant magnetoresistance (SV-GMR) sensor is proposed to estimate low concentration magnetic fluid content density inside the body in a minimal, low invasive way.

2. Principles of Hyperthermia Treatment

Lately hyperthermia has been shown to be a possible cancer therapy based on induction heating [4, 5]. The sensitivity of cancer cells to heat compared with healthy cells paves the way for effective cancer management using hyperthermia treatment. Dextran magnetite (DM) is a complex of dextran and superfine iron oxide particles, and this complex is stable as a colloid without aggregation or deposition in various solvents or serum [6]. As shown in Fig. 1, DM is injected into the affected area in the body and brought close to the cancerous cells.

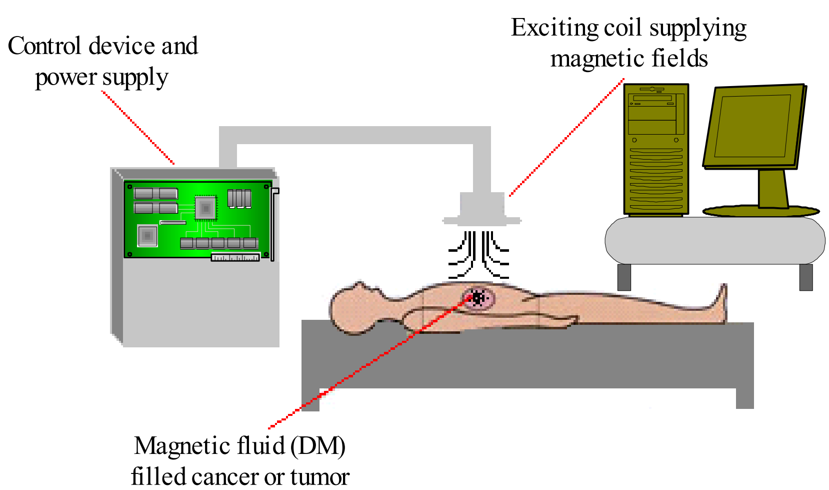

Fig. 1. Hyperthermia treatment as a cancer therapy.

The nano-particles heat up to around 42.5 °C due to the external AC magnetic fields that are acted upon the tumor [7]. Tumor tissues are heated directly since hysteresis loss is induced. Exposure to such heat for a given time will kill or partly destroy tumor tissue, where the latter can be utilized for giving low doses of other treatments such as X-ray therapy.

The heat capacity, Q (W/ml) generated by magnetite can be calculated as follows:

$$Q = k_m f D_w B^2 , \tag{1}$$

where f ; exciting frequency (kHz),
D_w; magnetic fluid weight density (mgFe/ml),
B ; applied magnetic flux density amplitude (T),
K_m; 3.14×103 (W/Hz/(mgFe/ml)/T^2/ml).

The value of the constant k_m was obtained by experiment, where an exciting magnetic flux at frequency 158 kHz was applied to Resovist®, a substance with a magnetic weight density of 28 mgFe/ml. It can be seen from Eq. (1) that all parameters except the magnetic fluid weight density (D_w) are generally known. When DM is injected into the affected area it spreads inside the cancer tissue effectively decreasing the magnetic fluid weight density [7-9]. So to control the heat in hyperthermia treatment it is important to verify D_w.

3. Analytical Estimation of Magnetic Fluid Content Density

3.1. Relationship between Relative Permeability and Magnetic Fluid Weight Density

The relative permeability of the magnetic fluid can be estimated by measuring the magnetic flux density in tissue injected with magnetic fluid. A relationship is established between the magnetic fluid weight density and relative permeability. Based on this relationship the magnetic fluid volume density, D_v, is calculated. The magnetic fluid weight density is estimated as

$$D_w = \frac{\gamma_f \times D_v}{(1 - D_v) + \gamma_f \times D_v} , \tag{2}$$

simplified and rearranged to obtain the magnetic fluid volume density as,

$$D_v = \frac{1}{1 + \left(\left(\frac{1}{D_w} \right) - 1 \right) \gamma_f} , \tag{3}$$

where γ_f = 4.58 (W-35 sample – Taiho Co.) and is the specific gravity of magnetic bead.

Magnetic nano-particles are assumed to have a cylindrical shape with equal height and diameter, and that they are uniformly distributed in the fluid. Furthermore, it is assumed that the nano-particles have an infinite permeability and water has one. Magnetic fluid density can be estimated based on the prediction of the magnetic field path when the fluid is placed under a uniform magnetic flux density. Two equivalent magentic paths, with and without magntic particles, are considered. Then an equation is obtained for the relative permeability derived from the equivalent magnetic permeance of one cubic meter [8,9]. So then the relative permeability, μ*, of magnetic fluid as a bulk is estimated as

$$\mu^* = 1 + 4D_V \approx 1 + 4D_W / \gamma_f \left(D_w << 1\right) \tag{4}$$

Eq. (4) shows that the shape and/or the size of magnetic particles have no effect on the relative permeability. Assuming the same equivalent path the equivalent relative permeability has the same expression even though the particle could be of spherical shape. The expression holds on the condition that the cavity includes a little amount of magnetic particle.

The electron microscopy of the magnetic fluid shows that the magnetic particles has a cluster structure as shown in Fig. 2(a). It was then assumed that the cluster of magnetite is distributed uniformly as shown in Fig. 2(b). It can be seen that there is some space in the cluster model and so we considered the space factor of spherical magnetite h_s [9]. So then the effective specific gravity is expressed as

$$\gamma_f' = h_s \gamma_f , \tag{5}$$

where h_s is 0.523. Eq. (4) can then be written as,

$$\mu^* = 1 + 4D_W / h_s \gamma_f \left(D_w << 1\right) \tag{6}$$

To verify Eq. (6) solenoidal shape vessels were filled with magnetic fluid of varying weight density. B-H curve tracer was used to measure the relative permeability. Fig. 3 shows the comparison of the results obtained by theory to experiments for a space factor of 0.523. It can be seen that the relative permeability is linearly proportional to the magnetic fluid weight density.

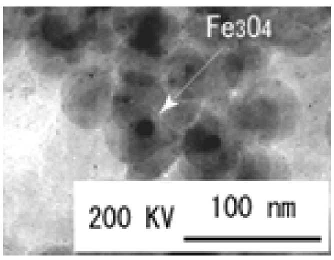

(a) Electron microscopy slide of magnetic fluid.

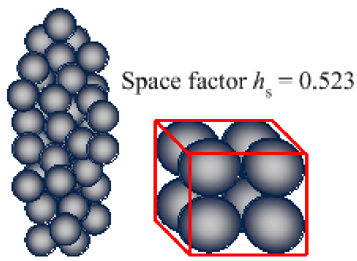

(b) Cluster model of magnetite.

Fig. 2. Microscopic model of magnetite.

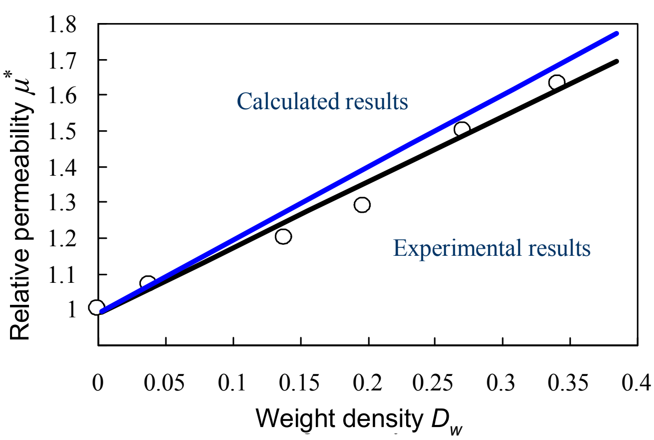

Fig. 3. Relative permeability vs weight density of magnetic fluid for space factor of 0.523.

3.2. Magnetic Flux Density Inside and Outside a Magnetic Fluid Filled Cavity under Uniform Magnetic Fields

Fig. 4 shows a magnetic fluid filled cavity placed under a uniform magnetic flux density. Flux lines will then concentrate at the magnetic fluid filled cavity, which is assumed to have permeability slightly greater than one.

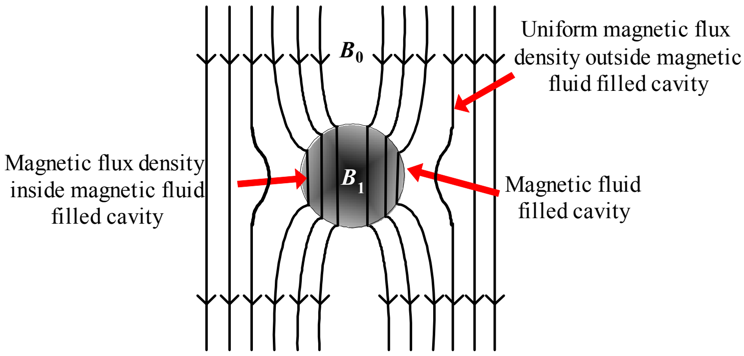

Fig. 4. Model showing magnetic flux distribution inside an embedded cavity.

If a magnetic flux, B_0, is applied then the flux in the cavity is assumed as B_1. The magnetic flux density inside the magnetic fluid filled cavity, B_1, will change according to the content density of the magnetic fluid.

The magnetic flux at the centre of the cavity, B_1, can be expressed according to the following equation:

$$B_1 = \frac{\mu^* B_0}{1 + N(\mu^* - 1)}, \tag{7}$$

where μ^* is the relative permeability which is assumed as slightly greater than 1 and N is the demagnetizing factor of the cavity. Substituting Eq. (4) for Eq. (7), we get,

$$\frac{B_1 - B_0}{B_0} \cong (1 - N)4D_v \tag{8}$$

From Eq. (8) it can be seen that from the difference between the applied flux, B_0, and the flux in the magnetic fluid, B_1, the volume density and thus the weight density of the magnetic fluid can be estimated. The change between the applied magnetic flux and the flux in the container is directly proportional to the magnetic fluid volume density.

3.3 Helmholtz Tri-coil and Uniform Magnetic Flux Density

Helmholtz coils are used in a variety of applications, primarily due to its ability to produce a relatively uniform field configuration, ease of construction and flexibility [10, 11]. Fig. 5 shows the designed Helmholtz tri-coil. The parameters are: a = 770 mm, b = 260 mm, c = 214 mm, h = 315 mm, N1, N2 and N3 are 140, 4 and 1 turns respectively. In biomedical applications low concentration magnetic fluid (typically less than 2.8 % weight density) is used. To clearly differentiate between magnetic fluid at low weight densities it is essential that the error from the midpoint in the uniform region is very low. The

Helmholtz tri-coil was designed to have an error less than or equal to 0.01 % 0.03 m in the axial and radial direction from the midpoint. Fig. 6 shows the analytical results obtained.

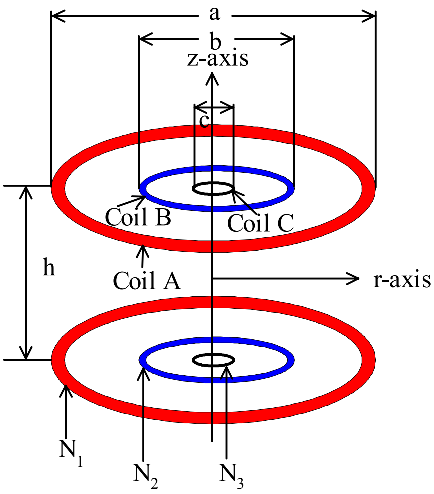

Fig. 5. Helmholtz tri-coil.

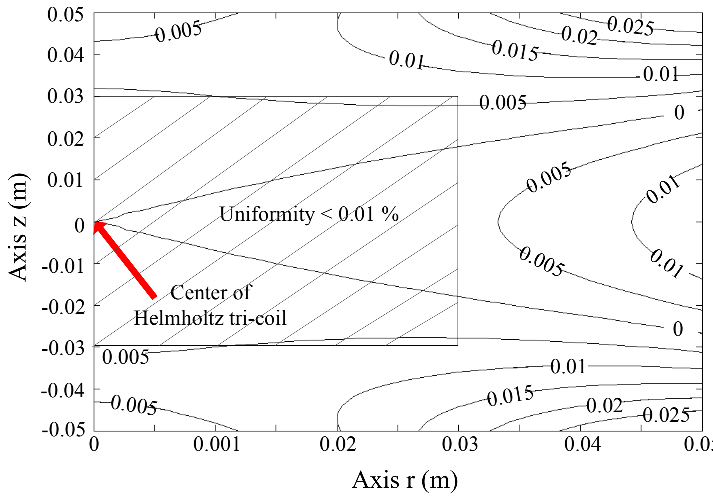

Fig. 6. Contour plot of error from the midpoint.

4. Numerical Analysis

Numerical analysis performed to analyze the magnetic flux density inside and outside a magnetic fluid filled cylindrical cavity is shown in Fig. 7. A two-dimensional (2-D) cross-section of the experimental setup is modeled, where the spatial coordinates are r and z. Since, it is possible to construct the 3-D geometry of the model by revolving the cross-section about an axis, with no variations in any variable when going around the axis of revolution, axial symmetry is used. Given that the cylindrical cavity is empty (no magnetic fluid present) then, the flux (B_1) inside the cavity is equal to the flux outside (B_0) the cavity. To simulate this condition permeability of 1 is given inside and outside the cavity, whereas permeability greater than 1 is given to simulate the condition of magnetic fluid inside the cavity. From the figure it is apparent that the magnetic flux lines are uniform at the cylindrical cavity and is perpendicular at the boundaries of the model, thus implying electric insulation.

The corresponding permeability value for each magnetic fluid weight density is used inside the cavity while outside the cavity permeability remains 1 (equal to air). So the magnetic flux density (B_1) inside the cavity changes with permeability, while the magnetic flux density outside the cavity (B_0) remains constant. Hence, for a given weight density and permeability of magnetic fluid the change in magnetic flux density inside and outside a cavity can be calculated.

Simulations were performed and the change in magnetic flux density calculated for a range of permeabilities that were used in actual experimentation. Fig. 8 shows the change in magnetic flux density with the penetration depth in the z axis. It can be observed that the change in magnetic flux density increases from the top of the cavity to the middle of the cavity, and there is symmetry about the middle of the cavity. Also the change in magnetic flux density from the cavity top to the center increases with increasing permeability. Fig. 9 shows the change in magnetic flux density in the r direction when z is 5 mm (at the center of the cavity). There is a slight change in the magnetic flux density as r increases from the center of the cavity. This increase is also proportional to the permeability of the cavity. This shows that the magnetic flux density is maybe not so constant in a cylindrical container as opposed to a true spherical or ellipsoidal cavity. Hence, the position of the sensor is of utmost importance and further analysis needs to be performed to evaluate this error. The change in magnetic flux density also drops rapidly at 8 mm. This is due to the fact that according to the cavity dimensions (height: 10 mm and radius: 8 mm) the position that the magnetic flux density drops rapidly is a boundary of the cavity.

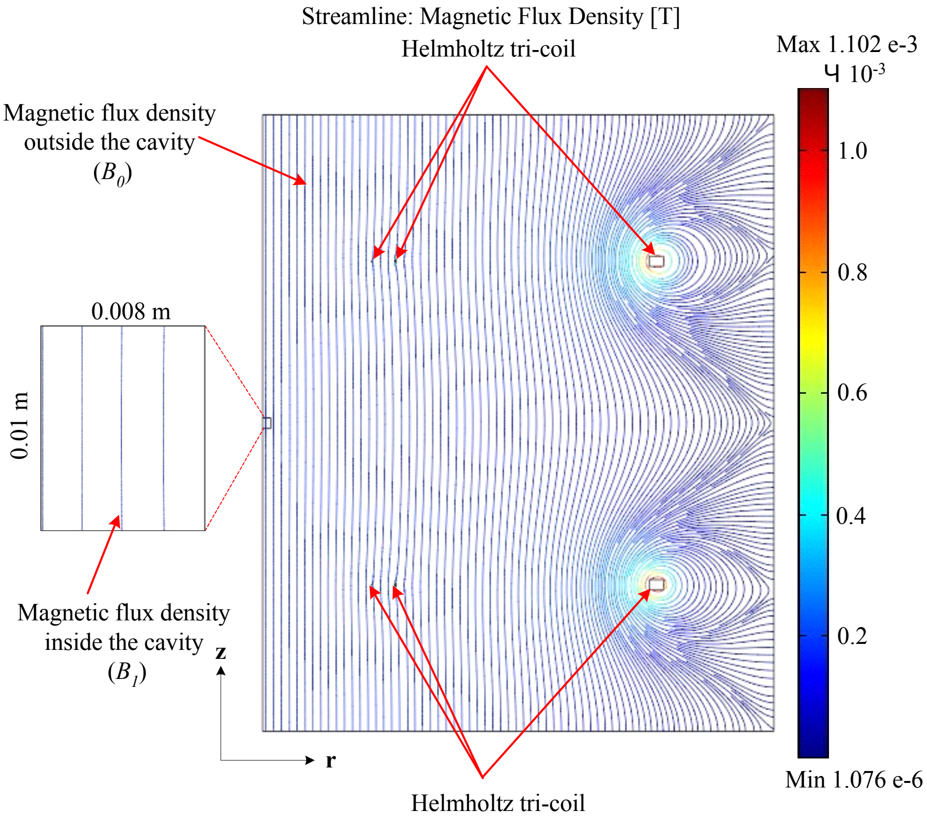

Fig. 7. FEMLAB simulation model.

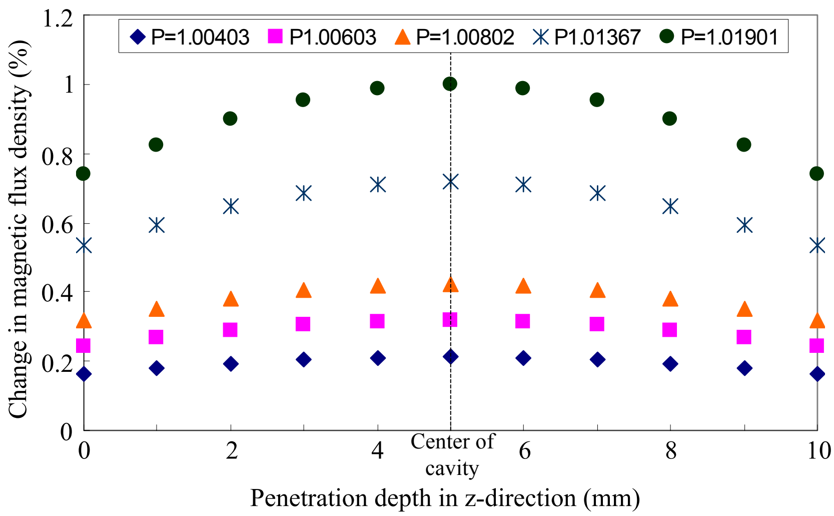

Fig. 8. Change in magnetic flux density in the z direction.

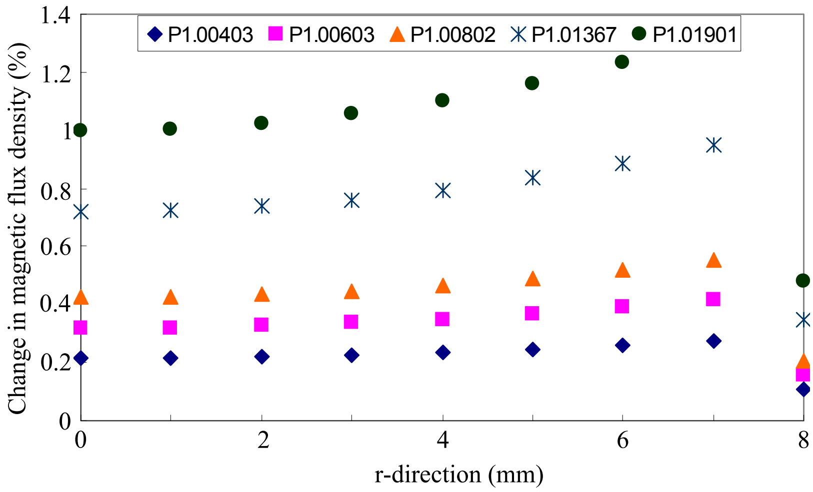

Fig. 9. Change in magnetic flux density in the r direction (from center of cavity).

5. Experimental Analysis

5.1. SV-GMR Sensor and Experimental Setup

The needle type SV-GMR sensor and the experimental setup used to estimate the magnetic fluid weight density is shown in Fig. 10. By measuring the applied flux density (outside of the cavity) and the magnetic flux density inside the magnetic fluid filled cavity the magnetic fluid weight density can be estimated. The SV-GMR sensor is especially fabricated for testing inside the body in a simple and a minimally low invasive way. The SV-GMR element with sensing area of 75 μm × 40μm is at the tip of the needle. The sensing direction is parallel to the needle. A constant current of 5 mA is applied to the SV-GMR sensor. The small signal characteristics of the sensor at 1 kHz is shown in Fig. 11. The sensitivity is approximately 12.5 μV/μT. Magnetic fluid is injected into cavity of 16 mm diameter and 10 mm height. The Helmholtz tri-coil is used to produce uniform magnetic flux of 100 μT at 100 Hz. The SV-GMR sensor needle tip is placed in the middle of the Helmholtz coil and the cavity is moved so that the needle tip is in the centre of the cavity.

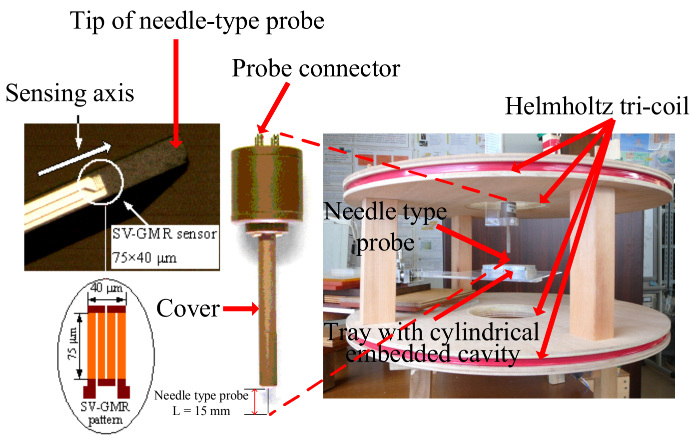

Fig. 10. Experimental setup.

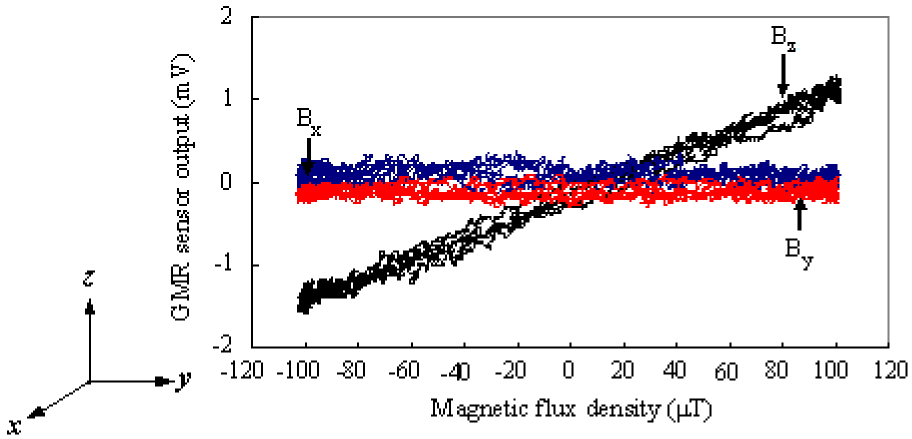

Fig. 11. Small signal ac characteristics of needle-type SV-GMR sensor at 1 kHz.

5.2. Estimation of Low Concentration Magnetic Fluid Weight Density

The volume density of DM used in medical applications such as in hyperthermia treatment is less than 1.2 %. So it is important to measure low concentration DM inside the body before as well as after treatment. Fig. 12 show the experimental results obtained. The relationship between the magnetic fluid weight density and the change in magnetic flux density is obtained. The relationship between the change in magnetic flux density and the magnetic fluid weight density is linear and proportional.

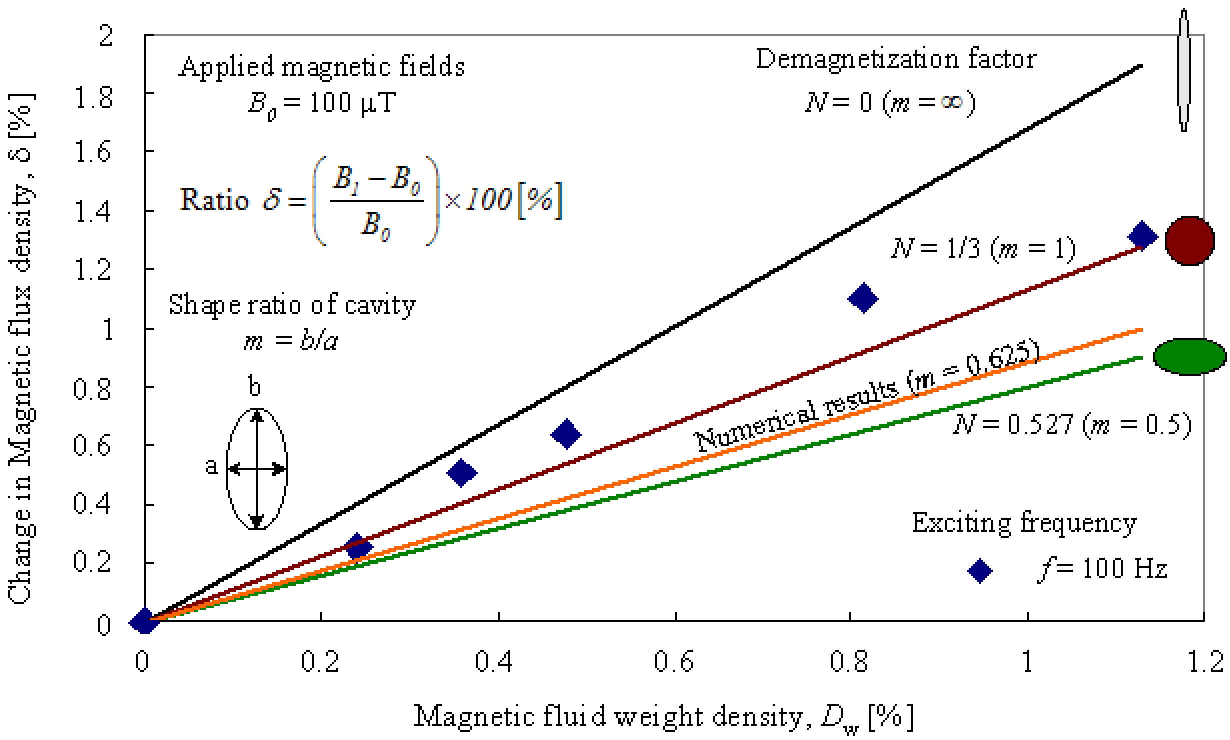

Fig. 12. Experimental results estimating low concentration magnetic fluid weight density.

5.3. Detection of Magnetic Fluid inside Agar

Experiments were performed to simulate potential in-vivo experimentation. A concentration of agar and magnetic fluid was made (5 % agar, 5 % magnetic fluid and 90 % distilled water) and cooled to solidify.

Then, potato starch was made and the solidified agar pieces were inserted into the potato starch as shown in Fig. 13. Experiments were performed with the needle-type SV-GMR sensor to estimate the magnetic fluid filled cylindrical agar pieces (diameter 16 mm and height 10 mm) that were inserted in potato starch. The demagnetizing factor of a cavity depends on the ratio of height to diameter of cavity (m). The sensor needle was applied to the middle of the agar pieces and the results are shown below in Fig. 14 for weight density percentages of 0.24, 0.36, 0.47 and 0.81. The result obtained here is only the amplitude of the signal corresponding to the magnetic flux density inside the magnetic fluid. The change in signal is the difference between the signal obtained inside the magnetic fluid and in potato starch (reference medium). It can be seen that the change in signal increases with increasing magnetic fluid weight density.

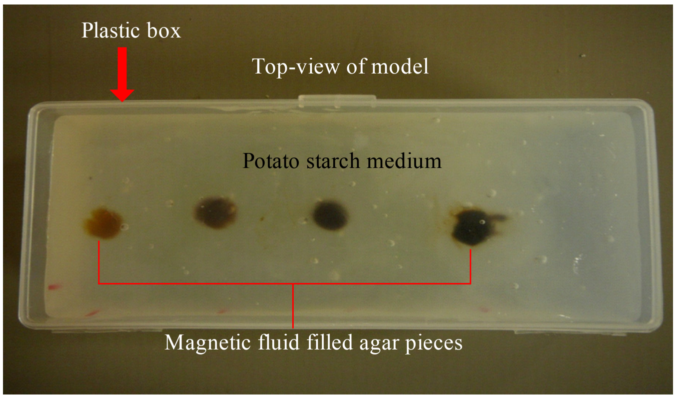

Fig. 13. Top-view model of magnetic fluid and potato starch.

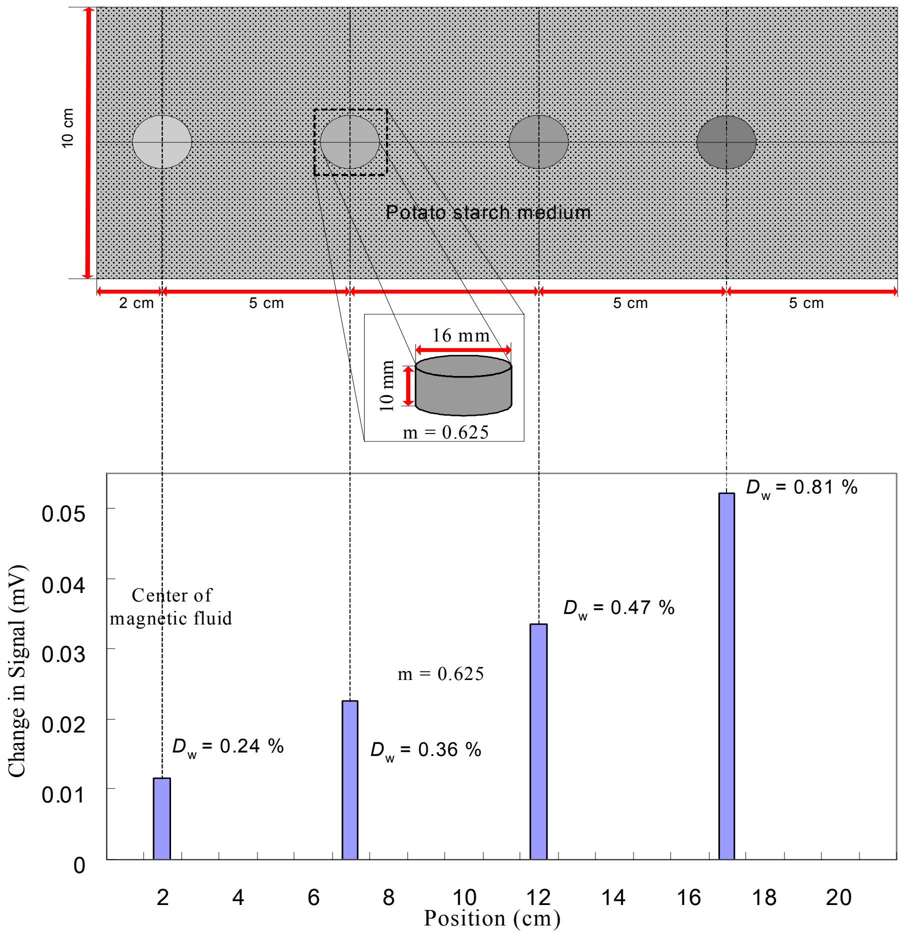

Fig. 14. Detection of magnetic fluid of varying densities.

Next, experiments were performed to verify Eq. (8). Eq. (8) shows that magnetic flux density inside and outside the cavity should only change with D_v. It can be seen that given the demagnetizing factor is the same the change in magnetic flux density is solely dependent on the magnetic fluid volume density. Shown in Fig. 15 are the results obtained for a range of weight densities for different sizes of magnetic fluid filled agar pieces (m = 0.625). It can be seen that for a given weight density and different sizes (where N is constant) there is not much difference between the change in signal. However, the change in signal increases with increasing weight density. For results obtained for m = 1 (D_w = 0.81 %) as shown in Fig. 16, the same diameters and positioning were used as in Fig. 15. The results show that change in signal do not vary so much between the four samples, verifying Eq. (8).

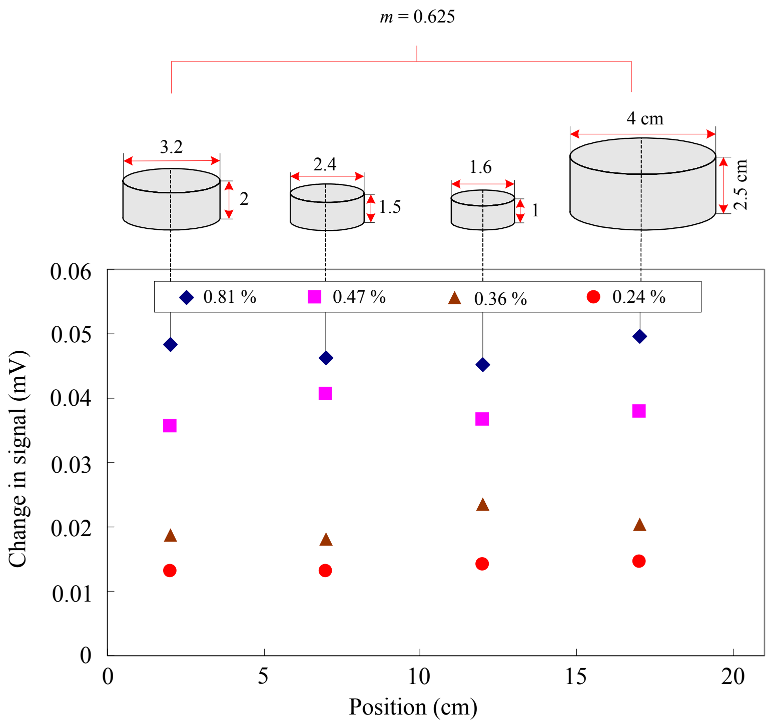

Fig. 15. Detection of magnetic fluid weight density (m = 0.625).

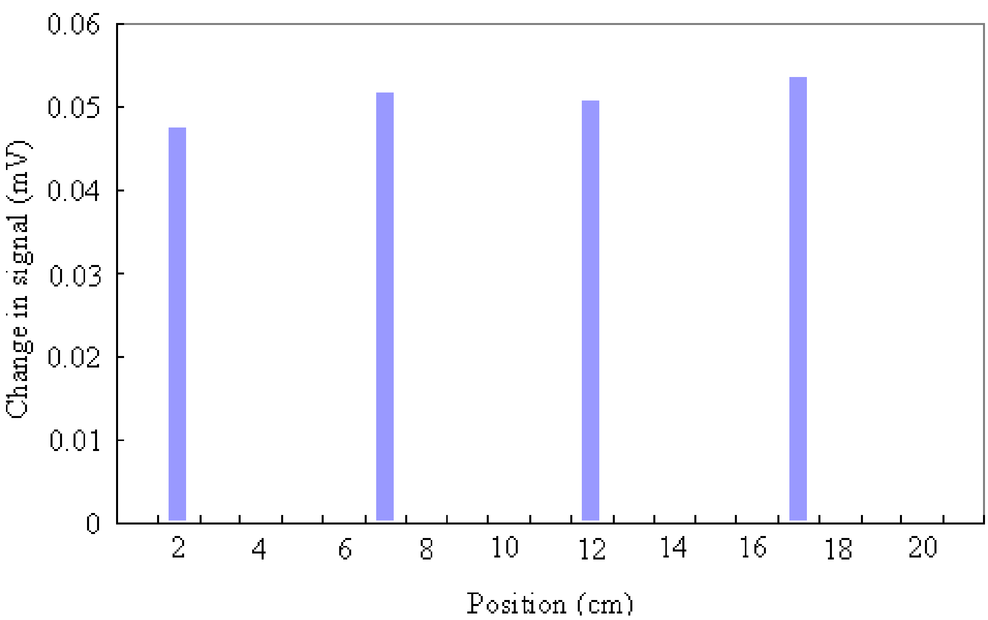

Fig. 16. Detection of magnetic fluid for weight density of 0.81 % (m = 1).

5. Conclusions

A novel needle type spin-valve giant magnetoresistance sensor is proposed for estimating the low concentration magnetic fluid weight density, which is prevalent in the biomedical field. The control of heat is critical in hyperthermia treatment so it is essential to verify the magnetic fluid weight density once inside the body before and after treatment. The relationship between the change in magnetic flux density inside and outside a magnetic fluid cavity has been shown by experimentation. Experiments were also performed to estimate magnetic fluid filled agar pieces inside potato starch reference medium. The experiments showed that magnetic fluid inside a reference medium can be estimated and shape of the cavity does not affect the magnetic flux density inside the magnetic fluid filled agar pieces. The results show that the proposed technique can be applied to biomedical engineering such as in the confirmation of magnetic fluid density injected into human body for cancer treatment by means of hyperthermia therapy, based on induction heating technique.

References

[1]. G. L. Cote, R. M. Lec, M. V. Pishko, Emerging Biomedical Sensing Technologies and Their Applications, *IEEE Sensors Journal*, Vol. 3, No. 3, June 2003, pp. 251-266.

[2]. M. H. Falk, R. D. Issels, Hyperthermia in Oncology, *International Journal of Hyperthermia*, 17, 1, Jan.-Feb. 2001, pp. 1-18.

[3]. J. van der Zee, Heating the patient: a promising approach ?, *Annals of Oncology*, 13, 8, August 2002, pp. 1173-1184.

[4]. R. Hergt, W. Andra, C. G. d'Ambly, I. Hilger, W. A. Kaiser, U. Richter, and H. G. Schmidt, Physical Limits of Hyperthermia Using Magnetic Fine Particles, *IEEE Transactions on Magnetics*, Vol. 34, No. 5, Sept. 1998, pp. 3745-3754.

[5]. K. Tazawa, I. Nagano, Development of a portable inductive heating system using dextran magnetite, *Journal of Hyperthermia Oncology Phys. D: Appl. Phys*. London, Vol. 19, Feb. 2003, pp. 79-85.

[6]. Nagano, H. Nagae, S. Shiozaki, I. Kawajiri, S. Ygitani, K. Katayama, and K. Tazawa, Development of a portable cancer treatment system using induction heating: a new weapon for killing the cancer, *2nd Kanazawa workshop*, Mar. 2006, pp. 11-15.

[7]. S. C. Mukhopadhyay, K. Chomsuwan, C. P. Gooneratne and S. Yamada, A novel needle-type SV-GMR sensor for bio-medical applications, *IEEE Sensors Journal*, Vol. 7, Issue 3, Mar. 2007, pp. 401-408.

[8]. S. Yamada, K. Chomsuwan, S. C. Mukhopadhyay, M. Iwahara, M. Kakikawa, and I. Nagano, Detection of Magnetic Fluid Volume Density with SV-GMR Sensor, *Journal of the Magnetics Society of Japan*, Vol. 31, No. 2, 2007, pp. 44-47.

[9]. C. Gooneratne, A. Lekawa, M. Iwahara, M. Kakikawa, and S. Yamada, Novel Needle Type GMR Sensor Application in Hyperthermia Therapy, *Proceedings of the 2nd International Conference on Sensing Technology (ICST 07)*, Nov. 26-28, 2007, Palmerston North, New Zealand, pp. 595-600.

[10]. J. Wang, S. She, S. Zhang, An improved Helmholtz coil and analysis of its magnetic field homogeneity, *Review of Scientific Instruments*, Vol. 73, No. 5, May 2002, pp. 2175-2179.

[11]. Sasada, Y. Nakashima, A planar coil system consisting of three coil pairs for producing uniform magnetic field, *Journal of Applied Physics*, Vol. 99, Issue 8, 2006, pp. 08D904 – 08D904-3.

Guide for Contributors

Aims and Scope

Sensors & Transducers Journal (ISSN 1726-5479) provides an advanced forum for the science and technology of physical, chemical sensors and biosensors. It publishes state-of-the-art reviews, regular research and application specific papers, short notes, letters to Editor and sensors related books reviews as well as academic, practical and commercial information of interest to its readership. Because it is an open access, peer review international journal, papers rapidly published in *Sensors & Transducers Journal* will receive a very high publicity. The journal is published monthly as twelve issues per annual by International Frequency Association (IFSA). In additional, some special sponsored and conference issues published annually.

Topics Covered

Contributions are invited on all aspects of research, development and application of the science and technology of sensors, transducers and sensor instrumentations. Topics include, but are not restricted to:

- Physical, chemical and biosensors;
- Digital, frequency, period, duty-cycle, time interval, PWM, pulse number output sensors and transducers;
- Theory, principles, effects, design, standardization and modeling;
- Smart sensors and systems;
- Sensor instrumentation;
- Virtual instruments;
- Sensors interfaces, buses and networks;
- Signal processing;
- Frequency (period, duty-cycle)-to-digital converters, ADC;
- Technologies and materials;
- Nanosensors;
- Microsystems;
- Applications.

Submission of papers

Articles should be written in English. Authors are invited to submit by e-mail editor@sensorsportal.com 6-14 pages article (including abstract, illustrations (color or grayscale), photos and references) in both: MS Word (doc) and Acrobat (pdf) formats. Detailed preparation instructions, paper example and template of manuscript are available from the journal's webpage: http://www.sensorsportal.com/HTML/DIGEST/Submition.htm Authors must follow the instructions strictly when submitting their manuscripts.

Advertising Information

Advertising orders and enquires may be sent to sales@sensorsportal.com Please download also our media kit: http://www.sensorsportal.com/DOWNLOADS/Media_Kit_2008.pdf